JJMIE

Volume 19, Number 3, Sep. 2025
ISSN 1995-6665
Pages 631– 639
https://doi.org/10.59038/jjmie/190315
Editor-in-Chief: Prof. Ali M. Jawarneh

Jordan Journal of Mechanical and Industrial Engineering

Analysis and Control of Vehicle-Driver Coupled System Post Tire Blowout: A Linear Quadratic Gaussian Approach

Ahmad Alshyyab[*1], Mahdi Al-Quran[2], Mohammad Arafa[2], Omar Nasleh[3]

[1] Aeronautical Engineering Department, Jordan University of Science and Technology, P.O. Box 3030, Irbid 22110, Jordan
[2] Department of Mechanical Engineering, The Hashemite University P.O. Box 330127, Zarqa,13133, Jordan
[3] Department of Mechatronics Engineering, The Hashemite University P.O. Box 330127, Zarqa,13133, Jordan

Received 12 Jun 2025 *Accepted 30 Jul 2025*

Abstract

To enhance the stability of the vehicle subjected to a tire blowout, this paper introduces a corrective active steering safety control system to stabilize the vehicle. The vehicle model is represented by a high-fidelity 14 degrees of freedom (DOF) model that is validated using MSC Adams Package. Subsequently, using the single-track bicycle control-oriented model, an active front steering control strategy in the framework of a linear quadratic regulator (LQR) controller combined with a Kalman filter is established and evaluated. To account for the possible driver reactions following the tire blowout accident, a driver model is augmented to the loop. This representation is more realistic in comparison with the open-loop-based controller design approach. The coupled vehicle-driver system is analyzed and integrated with the proposed linear quadratic gaussian (LQG) controller. The simulation results show that the proposed control system can sufficiently stabilize the system in the presence of the external disturbances associated with the tire blowout, as well as the reactions from the driver by means of minimizing the yaw rate triggered by these disturbances during both straight-line and cornering motions.

Keywords: Control of Vehicle; Kalman Filter; Linear Quadratic Gaussian; Post Tire Blowout; Vehicle-Driver Coupled System.

1. Introduction

Tire blowout is defined as the rapid and sudden deflation of the vehicle pneumatic tire. The inflation pressure dependent tire parameters are significantly affected following the blowout. Consequently, the vehicle body itself loses stability due to the couplings associated with the vehicle body-tire integrated system. As a result, the likelihood of the vehicle suffering from blowout being involved in a vehicular accident increases. As reported by the National Highway Traffic Safety Administration (NHTSA), 622 fatalities occurred in 2021 because of tire related crashes [1].

In order to predict the motion response of the vehicle to a tire blowout, researchers proposed time-dependent variations of specific tire properties throughout the blowout duration [2, Blyth]. This assumption was enhanced later to account for the camber angle [3], toe angle effect [4], vertical load redistribution, and self-alignment torque [5]. This reconstruction of the forces generated from the tire-ground interaction deteriorates the vehicle lateral stability according to several studies [2, 6].

On the other hand, several researchers relied on these proposed models to develop handling stability controllers to keep the vehicle inside the safe driving regime. Yue et al. [7], introduced hierarchical three stages automated hazard escaping controller to stabilize the vehicle travelling on expressway. Zhang et al. [8], developed a cooperative path tracking and stability control system for an autonomous vehicle under extreme driving conditions. Chen and his team conducted a sequence of studies to control the vehicle motion after experiencing a tire blowout [9, 10]. Other studies tackled the same problem via different combinations of steering, braking, suspension actuation mechanism [11- 14].

The previous controllers were designed based on a simplified linear single-track model. Therefore, to expand the validity of the safety controller to cover vehicle nonlinear regions, Al Quran [15, 16] designed a nonlinear stability control system using sliding mode control theory. Moreover, data-driven control/observer design techniques were utilized in the framework of tire blowout stabilization [17, 18].

It is well known that the driver has a vital role in the stability of the vehicle. In fact, the vehicle/driver integrated system is a more accurate representation of the physics of the moving compared to the vehicle isolated system. Recently, the authors investigated the effect of driver possible reactions on the vehicle stability and found that the driver's incorrect responses to a tire blowout event further deteriorate the stability of the vehicle [19]. To overcome the key limitations of the previous studies like designing the controller with respect to the vehicle open

* Corresponding author e-mail: asalshyyab@just.edu.jo.

loop system, as well as including the dynamics of the actuators, this paper introduces a deeper insight into the tire blowout problem in the context of the driver/vehicle closed loop coupled system. Explicitly, the primary contributions of this paper can be summarized as follows:

- A mathematical model for the driver is injected to the loop.
- An automatic control system based on LQG is designed for this coupled system the vehicle-driver-controller integrated system is analyzed.
- The proposed control strategy accounts for the dynamics of the actuator.

The remaining of the paper is divided into the following sections: section two introduces the vehicle system model and emphasize the risk of the tire blowout instability. Section three covers the control system design and highlights the effectiveness of having the controller to mitigate the consequences of the tire blowout threat. Finally, the last section summarizes the study and incorporates the concluding remarks.

2. Vehicle System Modeling

To highlight the effect of the tire blowout on a moving vehicle, the vehicle body, tire, and tire blowout need to be modeled. To begin with, the vehicle-tire coupled system is modeled with reference to Figure 1, then the tire blowout model will be introduced.

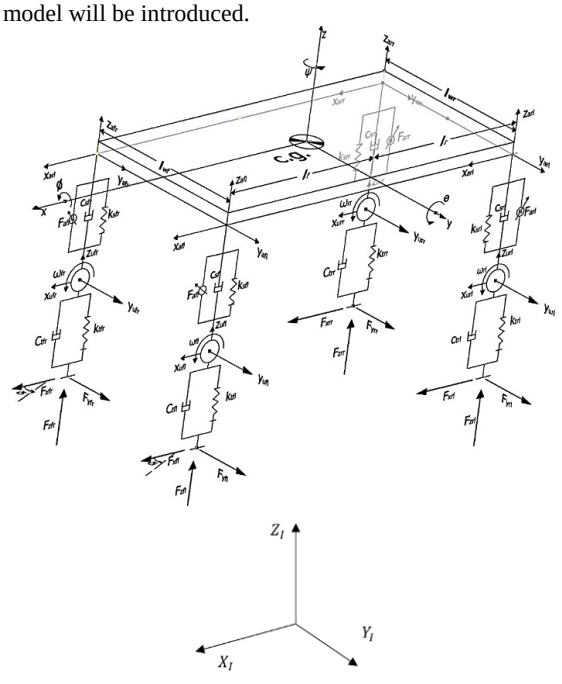

Figure 1. Vehicle full 14 DOF model

Figure 1 shows 14 degrees of freedom (DOF) vehicle model consisting of the vehicle body, suspension, and the wheels. The body has 6 DOF representing the vehicle translational motion along the body-fixed principal axes expressed by x, y, z as well as the rotational motions ϕ, θ, and ψ around the same axes. Each wheel has two degrees of freedom; namely, the vertical motion $z_{uij}$and the rotational motion ω_{ij} both measured from a coordinate system attached to the wheel center. In the previous terminology, the subscript *i* represents either front or and *j* refers to either left or right.

For the translation of the vehicle body, the conservation of linear momentum can be applied to get the following equations in a compact vectorial notation expressed in:

$$m\left({}^{V}\dot{v}_V + {}^{I}\omega_V \times {}^{V}\omega v_V\right) = \sum_{i,j=1}^{2} \left\{{}^{V}F_{sij} + {}^{V}F_{dij} + {}^{V}F_{arbij} + {}^{V}F_{tij}\right\} - m\,{}^{V}R_I \begin{bmatrix}0\\0\\1\end{bmatrix} g + {}^{V}F_{aero} + {}^{V}F_{inc}, \quad (1)$$

In the above equation, m is the mass of the vehicle body. ${}^{V}v_V$ is the velocity vector of the vehicle body center of mass relative to the body frame. ${}^{I}\omega_V$ represents the angular velocity of the chassis relative to the inertial frame. Furthermore, ${}^{I}R_V$ is the rotation matrix used to describe the motion of the vehicle body with respect to the reference ground frame and ${}^{V}R_I$ is its inverse.

On the other hand, the rotational dynamics can be derived using the conservation of angular momentum, which leads to the following equations:

The quantity in the matrix denotes the vehicle body inertia tensor. ${}^{V}r_{aij}$ refers to the position vectors of the pivot points at the body four corners expressed in the vehicle body-fixed frame. The definitions of the external loads as well as the main parameters used in this paper summarized in Table 1.

Table 1. Main parameters definitions

$\boldsymbol{\phi, \theta, and\ \psi}$	Vehicle roll, pitch, and yaw angles
$\boldsymbol{\beta}$	Vehicle sideslip angle
$\boldsymbol{C_a}$	Tire longitudinal stiffness
$\boldsymbol{C_b}$	Tire cornering stiffness
$\boldsymbol{C_r}$	Rolling resistance coefficient
$\boldsymbol{DOF}$	Degrees of freedom
${}^{V}\boldsymbol{F_{arbij}}$	Antiroll bar force
${}^{V}\boldsymbol{F_{aero}}$	Aerodynamic force
${}^{V}\boldsymbol{F_{dij}}$	Suspension damping force
${}^{V}\boldsymbol{F_{inc}}$	road loads from the inclination and bank angles
${}^{V}\boldsymbol{F_{sij}}$	Suspension spring force
${}^{V}\boldsymbol{F_{tij}}$	Tire forces from the interaction with the ground
$\boldsymbol{F_{zij}}$	Tire vertical force
$\boldsymbol{h}$	c.g. height
$\boldsymbol{I_x, I_y, I_z}$	Vehicle mass moment of inertia about principal axes
$\boldsymbol{J_{uyij}}$	Tire mass moment of inertia around spin axis
$\boldsymbol{k_t, C_t, s_u}$	vertical tire stiffness, damping of the tire, and the road inputs
$\boldsymbol{L_f}$	The distance from the c.g. to the front axle
$\boldsymbol{L_r}$	The distance from the c.g. to the rear axle
LQR	Linear quadratic regulator
LQG	Linear quadratic gaussian
$\boldsymbol{L_w}$	Track width
$\boldsymbol{m}$	Vehicle mass
$\boldsymbol{M_{aero}}$	Aerodynamic moment
$\boldsymbol{M_{rrij}}$	Rolling resistance moment
$\boldsymbol{\mu}$	Friction coefficient
$\boldsymbol{M_{uij}}$	Unsprung mass of the ijth corner of the vehicle
${}^{I}\boldsymbol{\omega_V}$	Vehicle angular velocity vector with respect to inertial frame
$\boldsymbol{R_w}$	Tire radius
${}^{V}\boldsymbol{r_{aij}}$	The position vector of the ijth tire relative to the vehicle frame
${}^{V}\boldsymbol{R_I}$	Rotation matrix from inertial frame to vehicle frame
$\boldsymbol{T_{bij}}$	Braking torque
$\boldsymbol{T_{dij}}$	Driving torque
${}^{V}\boldsymbol{v_V}$	Vehicle velocity vector with respect to vehicle frame
$\boldsymbol{y_u, z_u}$	Vehicle unsprung mass lateral and vertical positions

Figure 2 represents the free body diagram of the wheel. The vertical and spin motions are governed by the following equations:

$$m_{uij}\ddot{z}_{uij} = F_{zij} - F_{sij} - F_{dij} - F_{arbij} - m_{uij}g + k_{tij}s_{uij} + C_{tij}\dot{s}_{uij} \quad (3)$$

$$J_{uyij}\dot{\omega}_{yij} = T_{dij} - T_{bij} - r_{ij}F_{txij} - M_{rrij} \quad (4)$$

Where m_{uij} is the ij[th]unsprung mass of each corner. k_t, C_t, and s_u are the vertical tire stiffness, damping of the tire, and the road inputs the triggers the vertical motion, respectively.J_{uyij} is the mass moment of inertia of the ij[th] wheel about its spinning axis y_u while $\dot{\omega}_{yij}$ is its rotational acceleration.

The above equation are highly complex and coupled. Their full description can be found in reference [6] along with the kinematics and the expanded forms of several expressions.

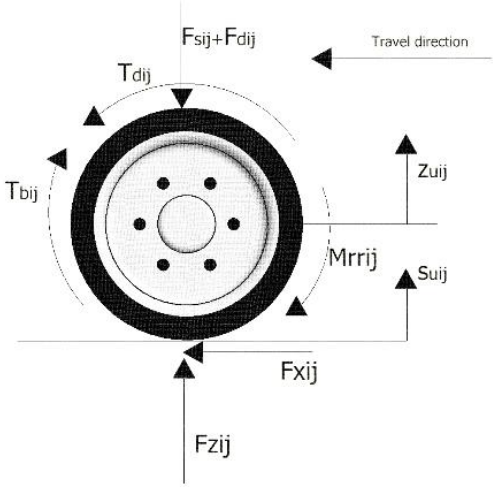

Figure 2. Wheel free body diagram

This model was previously verified by comparing its response to driver inputs to the response of the high-fidelity vehicle dynamics package MSC Adams as shown in Figure 3. From the figure, it is obvious that the derived mathematical model can replicate the MSC Adams results within an acceptable agreement. Then, the tire blowout model is incorporated to the vehicle system to highlight the risk of experiencing a tire blowout event as illustrated in Figure 4. The reader is encouraged to refer to reference [19] for more details about vehicle model and the effect of the blowout on the dynamics of the vehicle.

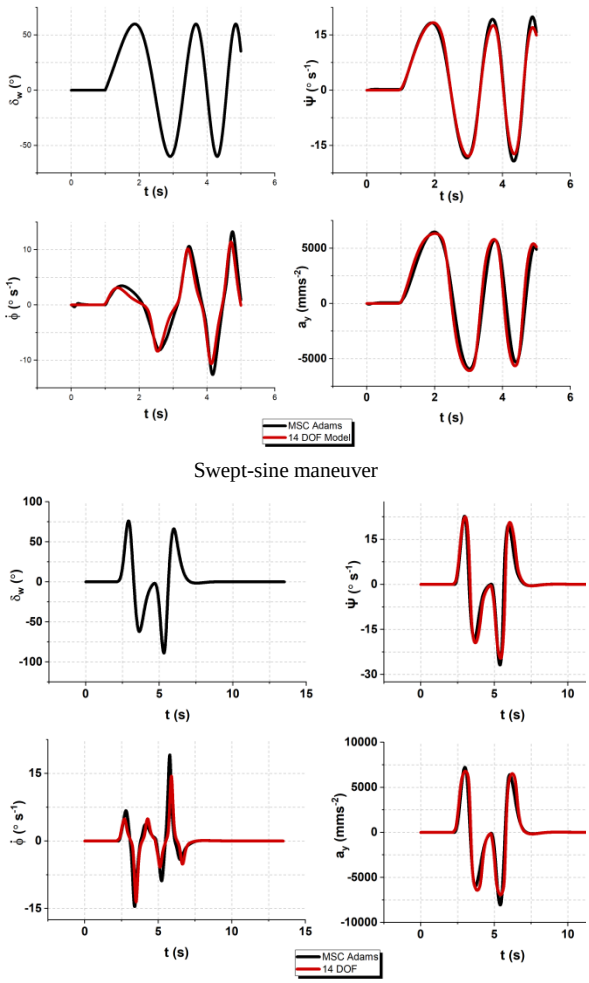

Figure 3. Vehicle model response compared with Adams/car response

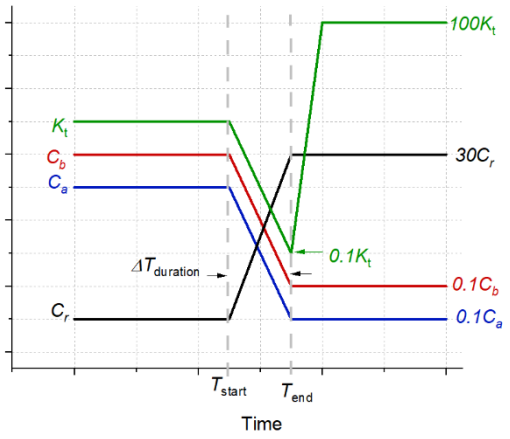

Tire parameters changes during air loss (C_a, C_b, are K_t are the tire longitudinal, cornering, and vertical stiffnesses, respectively)

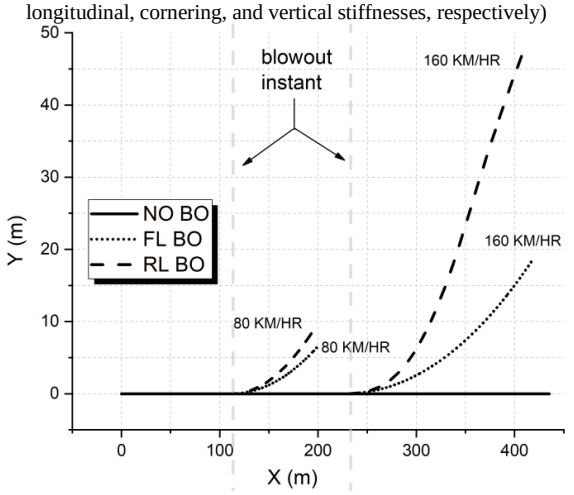

Vehicle trajectory in straight BO scenario

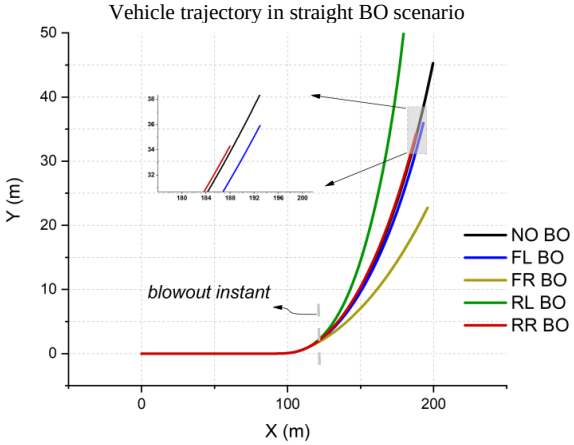

Figure 4. Tire blowout response

3. Control System Design

It has been observed that the vehicle suffering from a tire blowout will suffer from lane departure and/or understeering/oversteering and cannot be easily controlled by the average driver, or worse still, the driver may further deteriorate the stability by panic and wrong reactions. The objective of this section is to design a safety control system that keeps the vehicle tracking desired state trajectories when subjected to a tire blowout. Given the input steering from the driver and the vehicle speed, the controller calculates the desired yaw rate and side slip angle. Controller design is based on simplified vehicle and driver models which are selected to capture the essential parameters and the state variables for stabilization - sideslip angle and yaw rate. The well-known single-track vehicle model in Figure 5 used to synthesize the safety enhancement controller is formulated as [20]

$$\dot{x} = Ax + B\delta,\ y = Cx$$

$$x = \begin{bmatrix}\beta \\ \dot{\psi}\end{bmatrix}, y = \dot{\psi}$$

$$A = \begin{bmatrix} -\frac{2C_{bf}+2C_{ar}}{mv_x} & -1-\frac{2l_fC_{bf}-2l_rC_{br}}{mv_x{}^2} \\ -\frac{2l_fC_{af}-2l_rC_{br}}{I_z} & -\frac{2l_f^2C_{bf}+2l_r^2C_{br}}{I_zvx} \end{bmatrix},\ C = [0 \quad 1]$$

$$B = \left[\frac{2C_{bf}}{mvx} \quad \frac{2l_fC_{bf}}{I_z}\right]^T, \tag{5}$$

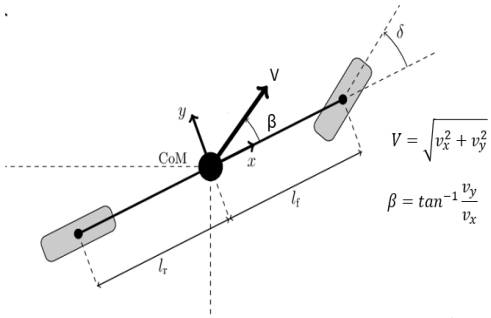

Figure 5. Vehicle single-track model

The determination of the target yaw rate and sideslip angle is derived from the steady state lateral motion of the single-track model and can be represented as [21]

$$\dot{\psi}_{target} = \begin{cases}\dot{\psi}_{des} & if\ |\dot{\psi}_{des}| \le \dot{\psi}_{upper_{bound}} \\ \dot{\psi}_{upper_{bound}} & if\ |\dot{\psi}_{des}| > \dot{\psi}_{upper_{bound}}\end{cases}$$

$$\dot{\psi}_{upper_{bound}} = 0.85\frac{\mu g}{v_x} \tag{6}$$

$$\dot{\psi}_{des} = \frac{v_x}{l_f + l_r + \frac{mv_x^2(l_rC_{ar} - l_fC_{af})}{2(l_f+l_r)C_{af}C_{ar}}}\delta$$

Where μ is the tire-road friction coefficient and

$$\beta_{target} = \begin{cases}\beta_{des} & if\ |\beta_{des}| \le \beta_{upper_{bound}} \\ \beta_{upper_{bound}}sgn(\beta_{des}) & if\ |\beta_{des}| > \beta_{upper_{bound}}\end{cases}$$

$$\beta_{upper_{bound}} = tan^{-1}(0.02\mu g) \tag{7}$$

$$\beta_{des} = \frac{l_r - \frac{l_fmV^2}{2C_{ar}(l_f+l_r)}}{(l_f+l_r) + \frac{mV^2(C_{ar}l_r - C_{af}l_f)}{2C_{ar}C_{af}(l_f+l_r)}}\delta$$

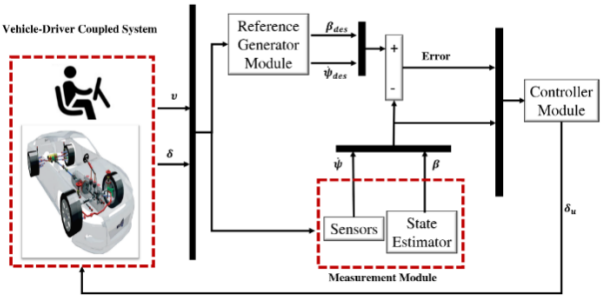

Figure 6. Controller block diagram

Figure 6 introduces the proposed control strategy as a block diagram. Within this framework, the Kalman filter supplies the estimated sideslip angle (which can't be easily measured directly) to the LQR controller in order to compute the control steering demand.

Firstly, a controller for a fixed velocity $x=const.$is considered. The states of the controller here are$x = [\beta \quad \dot{\psi}]^T$.The actuator is modeled as a first-order ordinary differential equation

$$\dot{\delta} = -K_a\delta + u \tag{8}$$

where the actual steering angle δ changes to the desired steering angle u after $3 \div K_a^{-1}$ seconds. Adding the actuator model to the model of the vehicle, we get

$$A_a = \begin{bmatrix} -\frac{2C_{bf}+2C_{ar}}{mv_x} & -1-\frac{2l_fC_{bf}-2l_rC_{br}}{mv_x{}^2} & \frac{2C_{bf}}{mvx} \\ -\frac{2l_fC_{af}-2l_rC_{br}}{I_z} & -\frac{2l_f^2C_{bf}+2l_r^2C_{br}}{I_zvx} & \frac{2l_fC_{bf}}{I_z} \\ 0 & 0 & -K_a \end{bmatrix}$$

$$B_a = \begin{bmatrix} 0 \\ 0 \\ 1 \end{bmatrix}, C_a = [0 \quad 1 \quad 0] \tag{9}$$

The driver is modeled according to [22] as

$$\tau_s\dot{u}_d(t) + u_d(t) = \frac{a_2v_x}{(a_1+l_f)}\varepsilon(t) + a_3\dot{\psi}(t) \tag{10}$$

where τ_s is the time delay of the driver's response, a_1, a_2, and a_3 are constants. $\varepsilon(t) = r(t) - \psi(t)$, and$r(t)$ is the desired angular orientation of the vehicle (the yaw angle). L is the look ahead distance. The signal$r(t)$ is generated from the curvature of the road and it is unknown. The state space representation of the driver is

$$\begin{bmatrix} \dot{u}_d \\ \dot{x}_i \end{bmatrix} = \begin{bmatrix} -\frac{1}{\tau_s} & -\frac{a_2v_x}{\tau_s(a_1+l_f+l_r)} \\ 0 & 0 \end{bmatrix}\begin{bmatrix} u_d \\ x_i \end{bmatrix} + \begin{bmatrix} \frac{a_3}{\tau_s} \\ 1 \end{bmatrix}\dot{\psi} + \begin{bmatrix} \frac{a_2v_x}{\tau_s(a_1+l_f+l_r)} \\ 0 \end{bmatrix} r \tag{11}$$

Where$x_i = \psi$ is the yaw angle that is estimated by the driver. We already have the derivative of the yaw angle in the state vector and it can be merged. The state space representation of the vehicle/driver model becomes

$$\dot{x}_{ad} = A_{ad}x_{ad} + B_{ad}u_{lqr} + Gr \tag{12}$$

where $x_{ad} = \left(\beta \;\; \dot{\psi} \;\; \delta \;\; u_d \;\; \psi\right)^T$is the extended state vector and $u_{lqr}$is the correction from the LQR controller for stabilization. Also,

$$A_{ad} = \begin{bmatrix} -\frac{2C_{bf}+2C_{ar}}{mv_x} & -1-\frac{2l_fC_{bf}-2l_rC_{br}}{mv_x{}^2} & \frac{2C_{bf}}{mvx} & 0 & 0 \\ -\frac{2l_fC_{af}-2l_rC_{br}}{I_z} & -\frac{2l_f^2C_{bf}+2l_r^2C_{br}}{I_zvx} & \frac{2l_fC_{bf}}{I_z} & 0 & 0 \\ 0 & 0 & -K_a & 1 & 0 \\ 0 & \frac{a_3}{\tau_s} & 0 & \frac{-1}{\tau_s} & \frac{a_2v_x}{\tau_s(a_1+l_f+l_r)} \\ 0 & 1 & 0 & 0 & 0 \end{bmatrix} \tag{13a}$$

$$B_{ad} = \begin{bmatrix} 0 \\ 0 \\ 1 \\ 0 \\ 0 \end{bmatrix} \quad G = \begin{bmatrix} 0 \\ 0 \\ \frac{a_2v_x}{\tau_s(a_1+l_f+l_r)} \\ 0 \\ 0 \end{bmatrix} \tag{13b}$$

This analytic form of the state-space equations can be used also for variable velocity of the vehicle, however then the systems becomes time variant.

So now define the cost function for the LQR in infinite time horizon and specify some values of Q and R, which may be tuned to achieve different performance of the controller. By solving the algebraic Riccati equation we get the following state feedback controller

$$u = 0.02\,\beta + 2.1\,\dot{\psi} + 5.7\,\delta + 0.5\,u_d + 3.1\psi \tag{14}$$

The yaw angleψ and its rate$\dot{\psi}$ are assumed to be directly measurable from the gyroscope and the magnitometer (compass) inertial measurement unit (IMU). Furthermore, the steering angle at the wheelsδ and the commanded steering angle by the driveru_d can be directly measured by the pulse encoders. The only unknown variable here is the sideslip angle β, which has to be estimated by an observer. A Kalman filter of the form

$$\hat{x}_{ad} = A_{ad}\hat{x}_{ad} + B_{ad}u + L(\vec{y} - C_{ad}\hat{x}_{ad}) \tag{15}$$

is assumed, where the measured output variables$\vec{y} = (\dot{\psi}, \delta, u_d, \psi)$ are compared with the respective calculated output variables from the model. The filter gain L is calculated such that it minimizes the expected value of the estimation error co-variance $P = E[(x_{ad} - \hat{x}_{ad})^2]$ and to guarantee unbiased estimate $\hat{x}_{ad} \to \hat{x}_{ad}$. The Kalman filter gain L satisfying the above conditions is selected as

$$L = A_{ad}PC_{ad}^T\left(C_{ad}P\,C_{ad}^T + R\right)^{-1} \tag{16}$$

where R is a positive definite matrix of the output noise covariance. It can be determined from the sensor specifications or by statistical experiments.

The state covariance matrix P is a positive definite solution of the following Riccati equation

$$A_{ad}^TPA_{ad} - A_{ad}^TPB(B^TPB + R)^{-1}B^TPA_{ad} + Q = 0, \tag{17}$$

where Q is positive definite matrix of state noise variance. It specifies the uncertainty of the initial state of the system. Next figures present the performance of the synthesized LQR controller with the Kalman filter.

Table 2. Tire and vehicle parameters used in the simulation

Vehicle mass	m	1527 kg
Vehicle mass moment of inertia about z axis	I_z	1340 kg.m2
The distance from the c.g. to the front axle	L_f	1.48 m
The distance from the c.g. to the rear axle	L_r	1.08 m
c.g. height	H	0.401 m
Track width	LW	1.56 m
Tire radius	Rw	0.326 m
Tire mass moment of inertia around spin axis	J_{uyij}	1 kg.m2
Friction coefficient	μ	0.9
Tire longitudinal stiffness	C_a	124619 N
Tire cornering stiffness	C_b	131780 N/rad
Rolling resistance coefficient	C_r	0.02
Driver model parameters	a_1, a_2, a_3	10, 0.1, 0.02
Driver reaction time	τ_s	0.2
Vehicle longitudinal velocity	v_x	80 km/hr

4. SIMULATION EXPERIMENTS

The performance of the synthesized controller is evaluated when it is applied to the nonlinear high-fidelity vehicle model. The nonlinear model accounts for nonlinear tire forces, driving and breaking torques. The simulation time is 20 seconds and tire blowout event is triggered in the 5th second of the experiment by sudden drop of Ca and

Cb, and sudden increase of Cr parameters of the front left tire throughout 0.1 second. It is assumed that this event occurs during a reference turn at 30 deg.

Table 2 presents the numerical values of the main vehicle and tire parameters used in the simulations.

Fig. 7 compares the step response of the closed-loop system with the driver alone and the closed-loop system with LQR which assists the driver in critical situations. As can be seen from the figure the LQR controller improves the performance of the steering by decreasing the settling time from 25 sec to 5 sec.

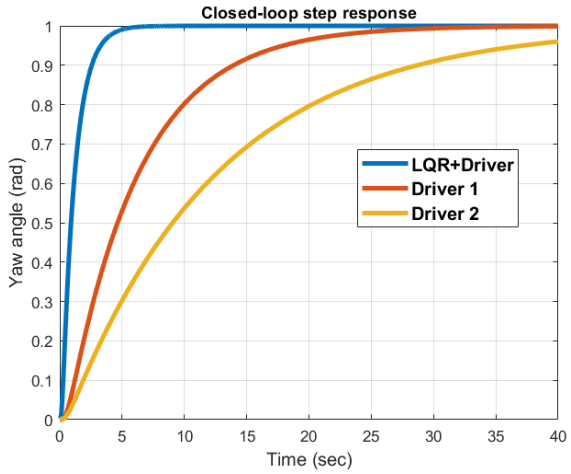

Figure 7. Step response of the closed-loop system with the LQR controller and the Kalman filter

Fig. 8 clearly demonstrates the difference in amplitudes of the resultant yaw angle deviation in case of tire blowout. It is evident that driver alone shows a considerable deviation in comparison to the case when driver reactions are assisted with the LQR controller. The amplitude of the deviations is reduced almost 10 times. Fig. 9 compares the steering command of the both control strategies. As can be seen the reaction of the driver is slower that the reaction of the system with the LQR controller. This is the main advantage of applying the assisting controller - to guarantee a smaller reaction time, which cannot be achieved by the driver especially in critical circumstances.

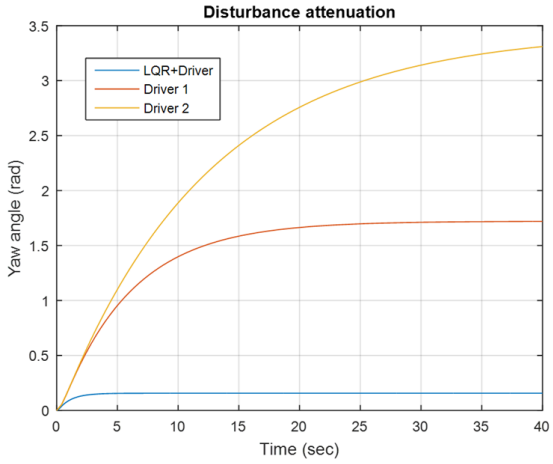

Figure 8. Reaction to constant disturbance applied to yaw rate

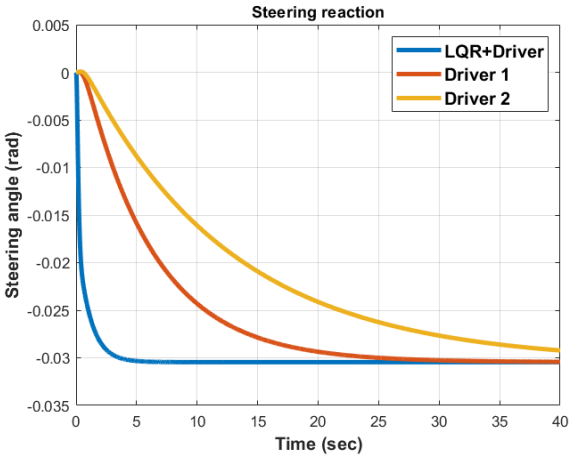

Figure 9. Control signal applied to the steering wheels.

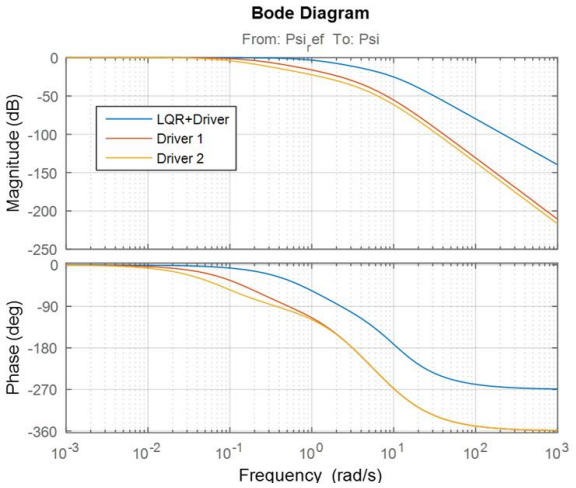

Figure 10. Closed-loop complementary sensitivity function

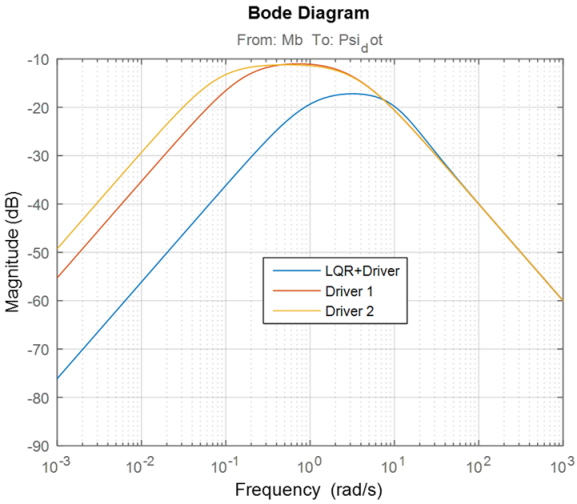

Figure 11. Sensitivity of the $\dot{\psi}$ to blowout disturbance

The frequency response of the system is examined in Fig. 10 and Fig. 11. Figure 10 compares the bandwidth of the system with the driver and with the LQR controller. It can be observed that when the LQR is introduced in the system the bandwidth is increased with almost one decade which guarantees the faster response and disturbance attenuation.

Figure 11 illustrates that the low frequency components of the blowout torque are attenuated more than 100 times

in case of the LQR controller and only 10 times in the case of the Driver without controller. The disturbance attenuation is guaranteed for whole frequency range. However, the resonance frequencies are different. For the LQR controller the resonance is at one decade to the right which means that amplitude of the vehicle instability will be lower.

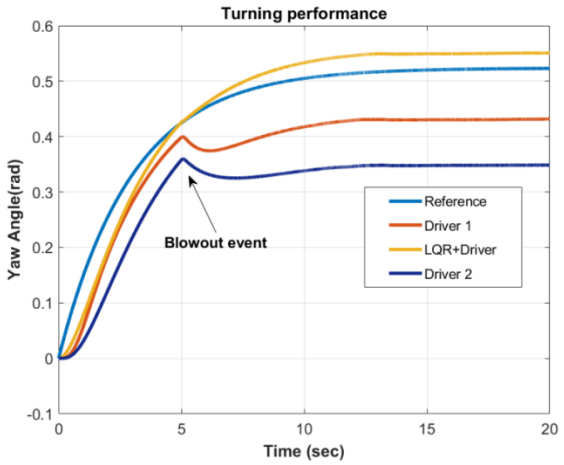

Figure 12. Reaction to blowout event of the driver and the LQR controller during a turn with the nonlinear model

Fig. 12 compares the performance of the closed loop system yaw angle between the driver alone and driver assisted with the designed LQR controller. As can be seen, the driver reaction is too slow, and he misses the turn. On the other hand, when the LQR controller is active, the desired yaw angle of the turn curve is more accurately followed despite the blowout event.

Fig. 13 reveals the control command for both controllers - driver alone and driver assisted with LQR. When the sudden blowout occurs, the reaction of the LQR controller is by far faster than the reaction of the driver, which is the cause for the improved performance during the turn.

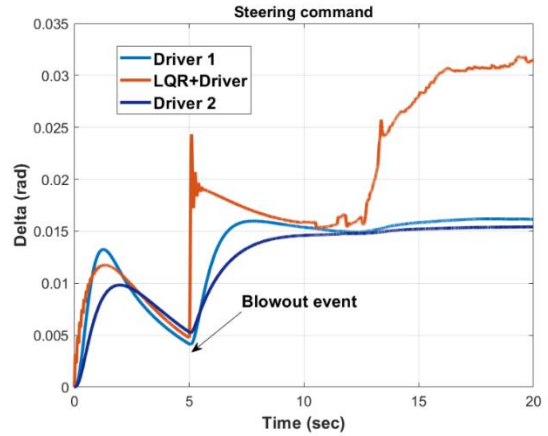

Figure 13. Control action applied to the steering wheels with the nonlinear model.

Figures 14 and 15 highlight the effectiveness of the proposed controller by diminishing the sideslip angle and the yaw rate disturbed by the blowout event. They clearly demonstrate how the responses approach their target values within a finite time. Finally, Figures 16 and 17 illustrate how the incorporation of the proposed controller has a stabilizing even in the presence of additional disturbances from the driver.

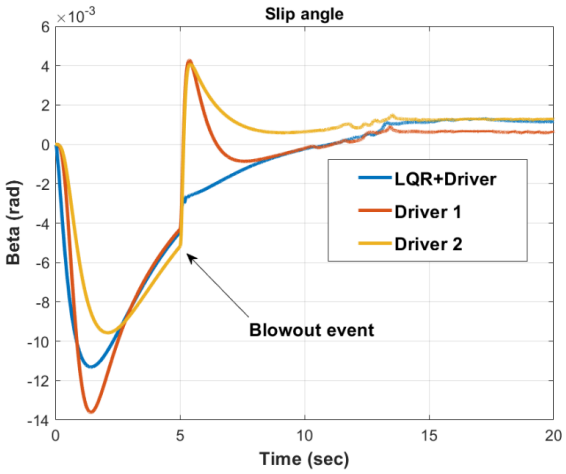

Figure 14. Slip angle during blowout event

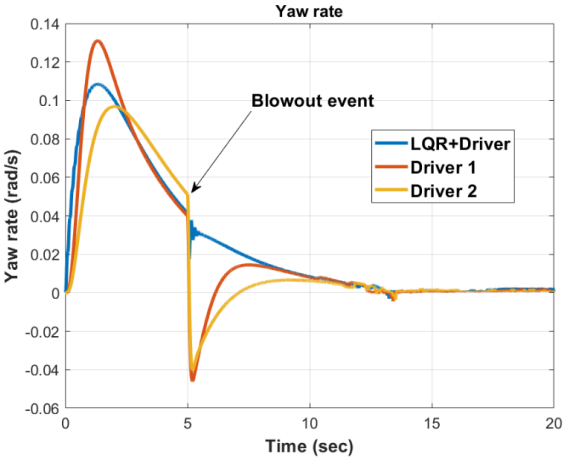

Figure 15. Yaw rate during blowout event

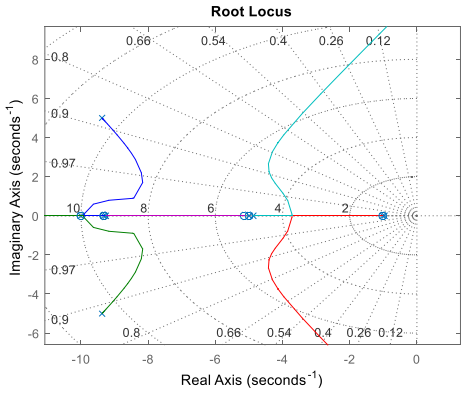

Figure 16. Root locus of the closed-loop system with LQR and the Driver

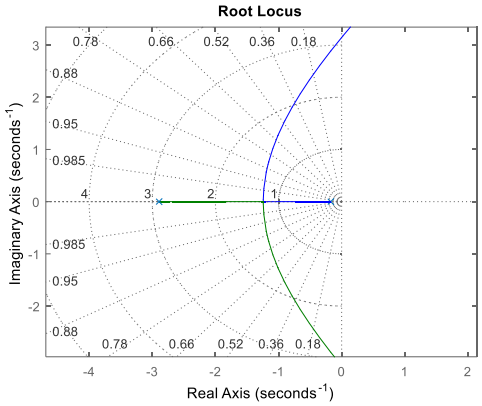

Figure 17. Root locus of the closed-loop system with the Driver

5. CONCLUSION

The problem of stability of a vehicle in an event of a sudden tire blowout is investigated and controlled in the paradigm of LQG controller. The objective is to stabilize the vehicle following a sudden loss of inflation pressure. A driver model reflecting the driver behavior is augmented to the vehicle system to account for his possible interventions. Moreover, the delays associated with the actuation are also accounted for. This representation is more realistic in comparison with the existing open loop systems. The resulting fifth order state space feedback gain is utilized to minimize a quadratic cost function of system state and control signal. The sideslip state is estimated by an optimal Kalman observer while the yaw rate is measured directly using sensors. The performance of the closed loop system is evaluated with the linear and nonlinear models with and without the driver. It is found that the proposed controller is perfectly competent to stabilize the vehicle and track the desired trajectory in straight line and cornering maneuvers when subjected to a tire blowout. Both the sideslip angle and yaw rate follow their target trajectories within a finite time. Future work is going to extend the current framework by exploring advanced control strategies like sliding mode controller and adaptive controller. Furthermore, this controller is going to be implemented and tested in hardware in the loop environment for further refinement.

References

[1] National Highway Traffic Safety Administration (NHTSA). https://www.nhtsa.gov/vehicle-safety/tires#resources

[2] W. Blythe, T. Day, and W. Grimes, "3-Dimensional Simulation of Vehicle Response to Tire Blow-outs," SAE Technical Paper 980221,1998,https://doi.org/10.4271/980221.

[3] X. Wang, L. Zang, T. Lv, Y. Li, "Dynamic characteristics of ISRFT blowout considering camber angle under typical driving conditions".Proceedings of the Institution of Mechanical Engineers, Part D: Journal of Automobile Engineering, Vol. 239 No. 2-3, 2023, pp 586-602. doi:10.1177/09544070231212791

[4] A. Li, Y. Chen, X. Du, and W.-C. Lin, "Should a Vehicle Always Deviate to the Tire Blowout Side?-A New Tire Blowout Model with Toe Angle Effects", *J. Dyn. Sys., Meas., Control*, Vol. 143, No. 10: 101008, 2021, https://doi.org/10.1115/1.4051034

[5] A. Li, Y. Chen, X. Du, and W.-C. Lin, "Enhanced Tire Blowout Modeling Using Vertical Load Redistribution and Self-Alignment Torque", ASME. *Letters Dyn. Sys. Control*. Vol. 1, No. 1, 2021, https://doi.org/10.1115/1.4046314

[6] M. Al Quran, and A. Ra'oufMayyas, "Three-Dimensional In-Depth Dynamic Analysis of a Ground Vehicle Experiencing a Tire Blowout," *SAE Int. J. Veh. Dyn., Stab., and NVH* Vol. 7, No. 4, pp 451-474, 2023, https://doi.org/10.4271/10-07-04-0030.

[7] M. Yue, L. Yang, H. Zhang *et al*, "Automated hazard escaping trajectory planning/tracking control framework for vehicles subject to tire blowout on expressway", *Nonlinear Dyn* Vol. 98, pp 61–74, 2019. https://doi.org/10.1007/s11071-019-05171-7

[8] Z. Zhang, L. Zheng, Y. Li, S. Li and Y. Liang, "Cooperative Strategy of Trajectory Tracking and Stability Control for 4WID Autonomous Vehicles Under Extreme Conditions", in *IEEE Transactions on Vehicular Technology*, vol. 72, No. 3, pp. 3105-3118, 2023, doi.1109/TVT.2022.3216486.

[9] A. Li, Y. Chen, W.-C. Lin, X. Du, "A Novel IDS-based Control Design for Tire Blowout",IFAC-Papers OnLine, Vol. 54, No. 20,2021, pp 179-184, https://doi.org/10.1016/j.ifacol.2021.11.172

[10] A. Li, Y. Chen, W. -C. Lin and X. Du, "A Novel Trust-Based Shared Steering Control for Automated Vehicles with Tire Blowout," *American Control Conference (ACC)*, San Diego, CA, USA, 2023,

[11] P.Sathishkumar, T. Jayaraman ,M. Thangaraj, "The tyre blow-out vehicle lateral pulling control using an active suspension system with comfort-lateral trajectory based control scheme". *Proceedings of the Institution of Mechanical Engineers, Part D: Journal of Automobile Engineering*, Vol. 238, No. 14, 2023, pp.4581-4595. https://doi.org/10.1177/09544070231197

[12] Y. Lu, Z. Han, J. Zhang, and Y. Li, "Collaborative control of trajectory tracking and braking stability of intelligent vehicles with a blowout tire." *J MechSciTechnol*, Vol. 38, 2024, pp.67–78. https://doi.org/10.1007/s12206-023-1206-y

[13] L. Yang, M. Yue, J. Wang and L. Guo, "Tire Blowout Motion Control of Over-actuated Ground Vehicles: A Hierarchical Framework," *2021 China Automation Congress (CAC)*, Beijing, China, 2021, pp.4950-4956. doi: 10.1109/CAC53003.2021.9727956

[14] L. Yang, K. Liu, H. Huang, Q. Liu, M. Gao and J. Wang, "Driver-automation collaborative steering control for intelligent vehicles under unexpected emergency conditions", *2022 IEEE Intelligent Vehicles Symposium (IV)*, Aachen, Germany, 2022, pp.1623-1630. doi: 10.1109/IV51971.2022.9827330.

[15] M. Al Quran, and A. Ra'oufMayyas, Design of a Nonlinear Stability Controller for Ground Vehicles Subjected to a Tire Blowout Using Double-Integral Sliding-Mode Controller", *SAE Int. J. Veh. Dyn., Stab., and NVH* Vol. 5, No. 3, 2021, pp.291-305. https://doi.org/10.4271/10-05-03-0020.

[16] M. Al-Quran and A. R. Mayyas, "A Nonlinear Tire Blowout Stabilizer Based on a Novel Integral Terminal Sliding Mode Controller," in *IEEE Access*, vol. 9, pp. 46652-46663, 2021, doi: 10.1109/ACCESS.2021.3067818.

[17] H. Chen and C. Lv, "RHONN-Modeling-Based Predictive Safety Assessment and Torque Vectoring for Holistic Stabilization of Electrified Vehicles," in *IEEE/ASME Transactions on Mechatronics*, vol. 28, no. 1, pp. 450-460, 2023. doi: 10.1109/TMECH.2022.3202076

[18] L. Yang, M.Yue, Y. Liu, L. Guo,"RBFNN based terminal sliding mode adaptive control for electric ground vehicles after tire blowout on expressway", Applied Soft Computing, Vol. 92, pp.106304. https://doi.org/10.1016/j.asoc.2020.106304.

[16] M. Al Quran, and A. Ra'oufMayyas, "Tree-Dimensional In-Depth Dynamic Analysis of a Ground Vehicle Experiencing a Tire Blowout," *SAE Int. J. Veh. Dyn., Stab., and NVH*, Vol. 7, No. 4, 2023, pp.451-474. https://doi.org/10.4271/10-07-04-0030

[17] Abe M, *Vehicle Handling Dynamics: Theory and Application*, 2nd ed. Oxford. Butterworth-Heinemann, 2015.

[18] Rajamani R.*Vehicle Dynamics and Control*, 2nd ed. New York, NY, USA: Springer, 2012.

[19] Song J. "Design and Comparison of AFS Controllers with PID, Fuzzy-Logic, and Sliding-Mode Controllers", Advances in Mechanical Engineering. Vol. 5. 2013. doi:10.1155/2013/401548